CMS Physics Analysis Summary

Contact: cms-pag-conveners-exotica@cern.ch 2012/03/09

Search for Resonances with the Dijet Angular Ratio

The CMS Collaboration

Abstract

A search for dijet resonances is performed using 2.2 fb^{-1} of proton-proton collision data at $\sqrt{s} = 7$ TeV recorded by the CMS detector at CERN. The study is based on the dijet angular ratio, the ratio of the number of events with the two leading jets having pseudorapidity difference $|\Delta\eta| < 1.3$ to the number of events with $1.3 < |\Delta\eta| < 3.0$. Models of new resonances which decay into two jets typically predict dijet angular distributions and hence, values of the dijet angular ratio which differ from standard model processes. We thus use the measurement of the angular ratio as a function of mass to set limits on the cross sections of new spin-$\frac{1}{2}$ quark-gluon resonances. We exclude excited quarks of mass less than 3.2 TeV at 95% confidence level, where a limit of 2.8 TeV is expected.

1 Introduction

Hard pp collisions at the CERN Large Hadron Collider (LHC) are dominantly characterized by the presence of jets arising from the scattering and subsequent fragmentation of quarks and gluons according to quantum chromodynamics (QCD). The angular distribution of jets is sensitive to new physics beyond the standard model, including processes involving a resonance that decays into two jets such as expected from an excited quark [1, 2]. The angular distribution of the two highest tranvserse momentum jets is sensitive to dijet resonances because QCD jets tend to be produced at forward angles, while most models of new physics involving a massive resonance decaying into a dijet give essentially isotropic angular distributions in the center of mass frame.

The Compact Muon Solenoid (CMS) and ATLAS have published direct searches for dijet resonances using the dijet mass distribution with 1 fb^{-1} [3, 4]. Here we present a search for dijet resonances with 2.2 fb^{-1} using the dijet angular ratio which is the ratio in signal-enriched and signal-depleted ranges of scattering angle. This search using angular information as a function of dijet mass is complementary to the previous searches which used only the dijet mass spectrum. A related CMS analysis with 2.2 fb^{-1} measured the angular distribution of dijets in a search for quark contact interactions [5], a non-resonant signal. A search by ATLAS with 36 pb^{-1} used a dijet angular ratio similar to the one in this analysis to search for dijet resonances [6].

2 Detector Description

A detailed description of the CMS experiment can be found elsewhere[7]. The CMS coordinate system has the origin at the center of the detector, the z-axis pointing along the direction of the counterclockwise-circulating proton beam of the LHC, with the transverse plane perpendicular to the beam. We define ϕ to be the azimuthal angle, θ to be the polar angle and the pseudorapidity as $\eta \equiv \frac{1}{2}\ln(\frac{|\vec{p}|+p_L}{|\vec{p}|-p_L}) = \ln(\tan[\frac{\theta}{2}])$ where p_L is the longitudinal component of momentum. The central feature of the CMS apparatus is a superconducting solenoid, of 6 m internal diameter, operating with a central field strength of 3.8 T. Within the field volume are the silicon pixel and strip tracker surrounded by the barrel and endcap calorimeters ($|\eta| < 3$): a high-granularity lead tungstate crystal electromagnetic calorimeter (ECAL) within a brass-scintillator hadronic calorimeter (HCAL). Outside the field volume, in the forward region, there is an iron-quartz-fiber hadronic calorimeter ($3 < |\eta| < 5$). The ECAL and HCAL cells are grouped into radially projective towers, for triggering purposes and to facilitate the jet reconstruction.

3 Jet Reconstruction

Jets are reconstructed using the anti-k_T algorithm [8] with size parameter $D = 0.7$. The reconstructed jet energy E is defined as the scalar sum of the calorimeter tower energies inside the jet. The jet momentum $\vec{p}$ is the corresponding vector sum: $\vec{p} = \sum E_i \hat{u}_i$ with $\hat{u}_i$ being the unit vector pointing from the primary vertex to the energy deposition E_i inside the jet. The jet transverse momentum p_T is the component of $\vec{p}$ in the transverse plane.

The E and $\vec{p}$ of a reconstructed jet are corrected for the non-linear response of the calorimeter [9]. The performance of the CMS detector with respect to jet reconstruction is described in detail in ref. [7].

4 Event Selection and Classification

Events are selected using single-jet triggers with varying thresholds on the jet p_T. Events are required to have at least one reconstructed primary vertex and the two jets with the largest p_T in the pseudorapidity range $|\eta| < 2.5$. The two leading jets must meet standard CMS jet-ID criteria [10].

The trigger can introduce a bias in the angular distributions, as central dijets will have a higher p_T than more forward dijets of the same mass. For each jet p_T trigger we therefore determine the dijet mass at which the trigger becomes fully (99.9%) efficient, and accept events selected by this trigger which have a higher mass. The fully efficient offline selection mass is determined for each trigger threshold independently.

Selected events are classified either as *inner* if the two leading jets' pseudorapidity separation $\Delta\eta$ is in the range $|\Delta\eta| < 1.3$ or as *outer* if the separation is in the range $1.3 < |\Delta\eta| < 3.0$. The analysis is then based on the ratio of inner to outer events (R). The resulting event counts are shown in Fig. 1 as differential dijet mass spectra. The dijet mass bin widths used are the same as those in the previous CMS search for dijet resonances [3] and are approximately equal to the dijet mass resolution. Dijets of mass 1770 GeV and higher enter the analysis through unprescaled triggers.

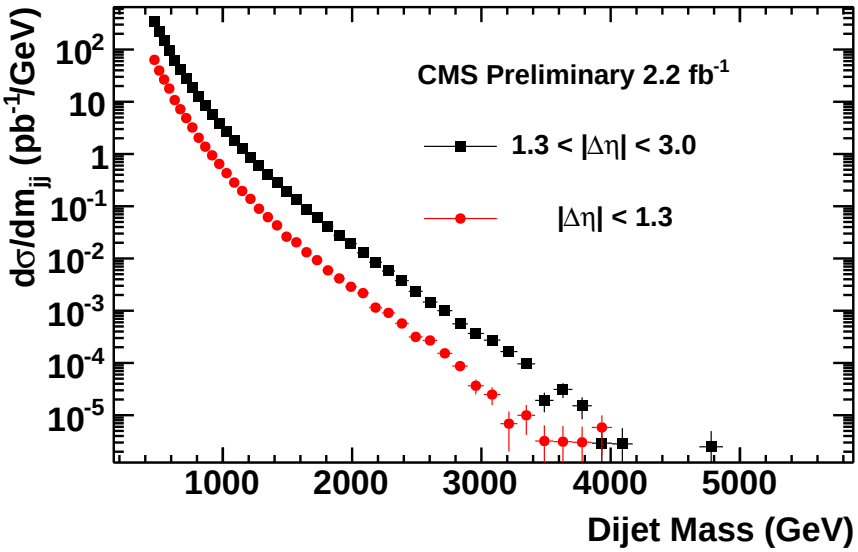

Figure 1: Differential dijet mass spectrum for inner and outer dijets used to measure the dijet angular ratio.

5 Dijet Angular Ratio

Figure 2 shows the measured dijet angular ratio R. The QCD prediction from PYTHIA 6.4 using the D6T tune [11] for R is shown as a solid line. The PYTHIA QCD prediction shown in Fig. 2 has been offset to fit a low dijet mass sideband, 500-600 GeV. The offset is needed because a leading-order prediction lacks hard gluon radiation, and the resulting angular distributions systematically underestimate the small-$|\Delta\eta|$ dijet production of QCD. In the sideband mass region the result of the fit to the data for the additive offset (0.019 ± 0.0019) is about 10% of the

value of R in data. Also shown in Fig. 2 are the expectations for an excited quark of mass 1.0, 1.5, and 2.5 TeV.

In Fig. 3 we show the difference between the data and the offset QCD predictions, divided by the statistical uncertainty on the data. With respect to a flat line at zero, this distribution has a χ^2/ndf of 41/39.

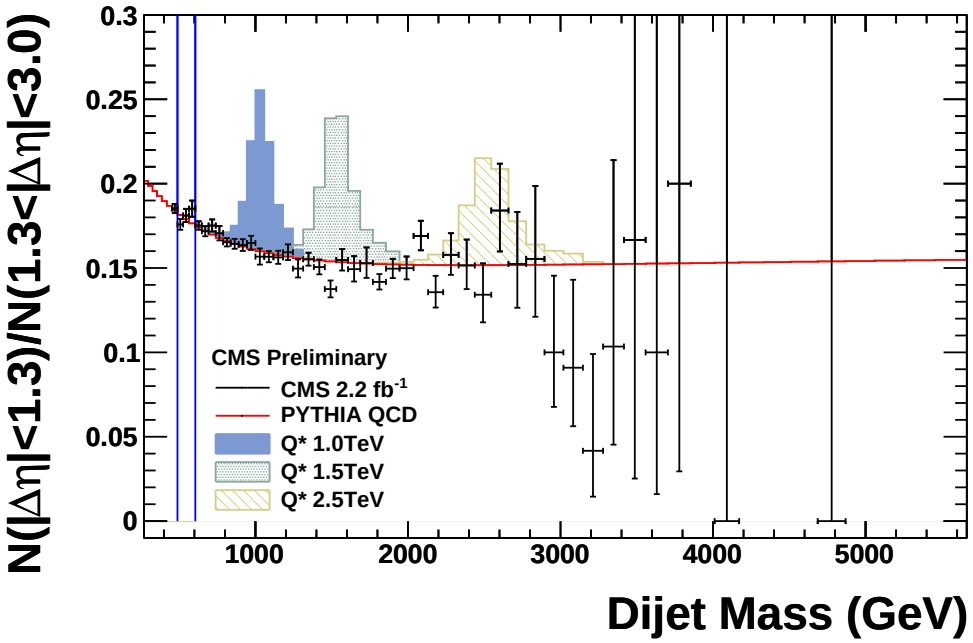

Figure 2: Dijet angular ratio from 2.2 fb^{-1} of integrated luminosity. The ratio is compared to predictions for PYTHIA QCD (red curve) normalized to the mass region 500-600 GeV (blue lines) and excited quark resonances with masses of 1.0, 2.5 and 2.5 TeV.

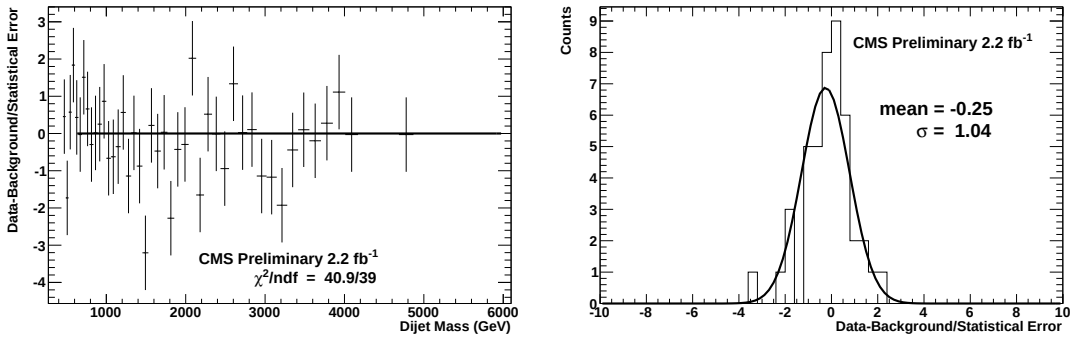

Figure 3: (Left) The data minus background divided by data statistical uncertainty of the measured dijet angular ratio. The fit to a flat line at zero is shown. (Right) The difference between the data and the QCD predictions, normalized by its statistical uncertainty.

5.1 Results

To test for the presence of new physics in the dijet angular ratio, we define the total likelihood over all dijet mass bins as the product of bin likelihoods $\mathcal{L}_j$, such that

$$\ln \mathcal{L} = \sum_{\text{bins}} \ln \mathcal{L}_j. \quad (1)$$

The log likelihood ratio $R_{ln\mathcal{L}}$ given predictions for QCD and each alternate hypothesis (QCD plus dijet resonance of a particular mass and cross section) is then written as

$$R_{\ln \mathcal{L}} = \ln \mathcal{L}_{\text{alt}} - \ln \mathcal{L}_{\text{QCD}}. \quad (2)$$

We compare the value of $R_{ln\mathcal{L}}$ in the data to distributions of the expected values under the two hypotheses, obtained in ensembles of pseudoexperiments, to set exclusion bounds with the CL_s criterion [12, 13].

We add the offset described above to the PYTHIA prediction to obtain the background expectation. We compare the measured angular ratio for dijet masses above 600 GeV to the background expectation to search for evidence of new physics.

The fact that this analysis is based on a ratio leads to the cancellation of some systematic uncertainty. Although it partially cancels in the ratio, the source of largest remaining systematic uncertainty in the measurement of R comes from the relative jet energy scale uncertainty between the inner and outer regions. We determine the uncertainty on the jet energy scale using test beam data, Monte Carlo simulation, and in-situ measurements [9]. To study the effect of this uncertainty on the dijet angular ratio, we vary the jet energy by plus or minus one standard deviation and observe the change in measured R to range from 0.07% at 800 GeV to 4% at 5500 GeV. Comparing the background expectation shown in Fig. 2 and the next-to-leading-order prediction of fastNLOv2 [14] and NLOJet++ 4.1.3 [15, 16] with CTEQ6.6 parton distribution functions [17] and renormalization and factorization scales set at the average of the two jet p_Ts, we find a systematic uncertainty on the background model which ranges from 3.4% above to 1.2% below our nominal background expectation. The comparison to NLO is carried out after correcting the NLO for non-perturbative effects, which are estimated in PYTHIA as the effect of switching on hadronization and multiple parton interaction in the D6T PYTHIA tune. The corrected NLO prediction is not normalized, yet closely follows the offset background prediction from PYTHIA.

These systematic uncertainties on the background expectation are independent of other important uncertainties, notably the statistical errors in each mass bin and an uncertainty on the offset added to the background prediction, which is less than 1% of the measured quantity. We also account for a 2.2% dijet mass uncertainty due to jet energy scale uncertainty, which would shift the signal peak, and a 4.5% uncertainty on the luminosity which affects the precision at which we can state cross section limits. All systematic uncertainties enter the ensembles as nuisance parameters that affect the ratio of inner to outer events expected in each dijet mass bin.

The data are consistent with the background expectation, and are used to determine 95% C.L. limits on the cross section as a function of dijet mass. Figure 4 shows the resulting limit as cross section multiplied by branching fraction and acceptance in picobarns for the benchmark q* model as a function of the resonance mass, as well as the 95% confidence level exclusion points for the data and the expected limits versus the resonance mass. The expected limit is at 2.85 TeV and the observed limit is at 3.20 TeV.

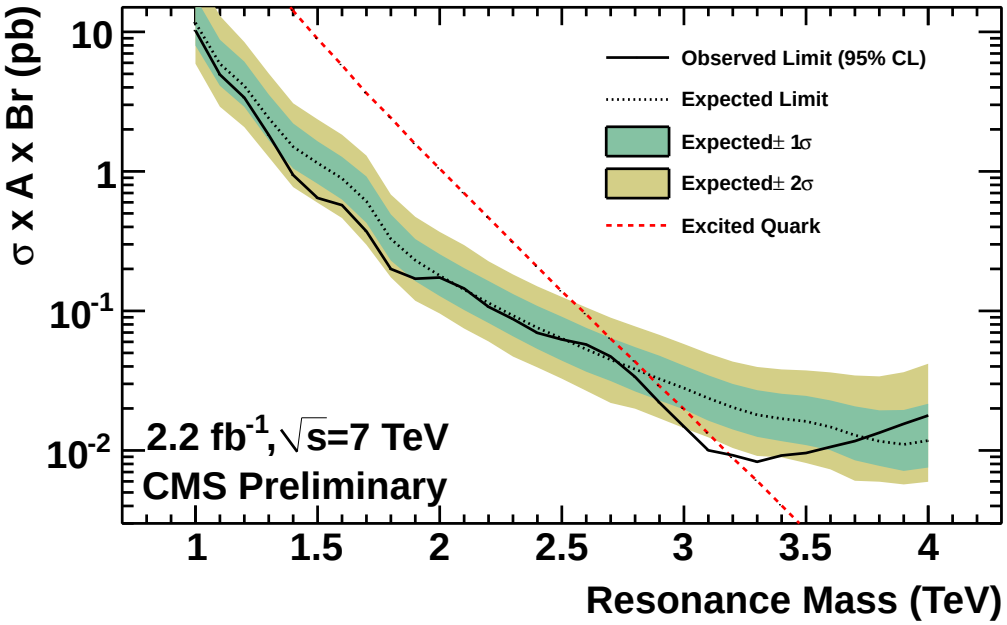

Figure 4: The observed 95% confidence level upper limits on $\sigma \times$ Acceptance $\times$ Branching Fraction for quark-gluon resonances with spin-$\frac{1}{2}$ (solid curve) and the expected limits (dashed curve) with their statistical and systematic variations at the 1σ and 2σ levels (shaded bands) are compared to the theory prediction for excited quarks (red dashed curve).

6 Conclusion

We present here the first results from the CMS experiment searching for resonances using the dijet angular ratio of inner events ($|\Delta\eta| < 1.3$) to outer events ($1.3 < |\Delta\eta| < 3.0$). We use a data sample corresponding to 2.2 ± 0.2 fb^{-1} of integrated luminosity from 7 TeV proton-proton collisions at the LHC. The dijet angular ratio observed in data agrees with the background expectation and there is no evidence for dijet resonances. We exclude an excited quark of mass less than 3.20 TeV at 95% C.L., where the expected limit is 2.85 TeV. This limit can be compared to the published limits with 1 fb^{-1} from CMS[3] (2.68 TeV expected, 2.49 TeV observed) and ATLAS[4] (2.81 TeV expected, 2.99 TeV observed).

References

[1] U. Baur, M. Spira, and P. M. Zerwas, "Excited-quark and -lepton production at hadron colliders", *Phys. Rev. D* **42** (Aug, 1990) 815–824. doi:10.1103/PhysRevD.42.815.

[2] U. Baur, I. Hincliffe, and D. Zeppenfeld, "Excited-quark and -lepton production at hadron colliders", *Int. J. Mod. Phys.* **A2** (1987) 1285.

[3] CMS Collaboration, "Search for resonances in the dijet mass spectrum from 7 TeV pp collisions at CMS", *Physics Letters B* **704** (2011), no. 3, 123 – 142. doi:10.1016/j.physletb.2011.09.015.

[4] ATLAS Collaboration, "Search for New Physics in the Dijet Mass Distribution using $1 fb^{-1}$ of pp Collision Data at $\sqrt{s} = 7TeV$ collected by the ATLAS Detector", *Physics Letters B* **708** (2011), no. 12, 37 – 54. doi:10.1016/j.physletb.2012.01.035.

[5] CMS Collaboration, "Search for quark compositeness in dijet angular distributions from pp collisions at $\sqrt{s}$ = 7 TeV", *Submitted to JHEP* (2012) arXiv:1202.5535.

[6] ATLAS Collaboration Collaboration, "Search for New Physics in Dijet Mass and Angular Distributions in pp Collisions at $\sqrt{s} = 7$ TeV Measured with the ATLAS Detector", *New J.Phys.* **13** (2011) 053044, arXiv:1103.3864. doi:10.1088/1367-2630/13/5/053044.

[7] CMS Collaboration, "The CMS experiment at the CERN LHC", *JINST* **3** (2008) S08004. doi:10.1088/1748-0221/3/08/S08004.

[8] M. Cacciari, G.P. Salam, and G. Soyez, "The anti-k_T jet clustering algorithm", *JHEP* **04** (2008) 63.

[9] CMS Collaboration, "Determination of Jet Energy Calibration and Transverse Momentum Resolution in CMS", *JINST* **6** (2011) P11002, arXiv:1107.4277. doi:10.1088/1748-0221/6/11/P11002.

[10] CMS Collaboration, "Jet Performance in pp Collisions at $\sqrt{s}$=7 TeV", *CMS Physics Analysis Summary* **CMS-PAS-JME-10-003** (2010).

[11] T. Sjöstrand, S. Mrenna, and P.Z. Skands, "PYTHIA 6.4 Physics and Manual", *JHEP* **05** (2006) 026.

[12] A. L. Read, "Presentation of search results: the CL_s technique", *Journal of Physics G: Nuclear and Particle Physics* **28** (2002), no. 10, 2693.

[13] T. Junk, "Confidence level computation for combining searches with small statistics", *NIM A* **434** (1999), no. 23, 435 – 443.

[14] T. Kluge, K. Rabbertz, M. Wobisch, "fastNLO: Fast pQCD Calculations for PDF Fits", arXiv:0609285v2.

[15] Z. Nagy, "Three-jet cross sections in hadron hadron collisions at next-to-leading order", *Phys. Rev. Lett.* **88** (2002) 122003.

[16] Z. Nagy, "Next-to-leading order calculation of three-jet observables in hadron-hadron collision", *Phys. Rev. D* **68** (2003) 094002.

[17] P. M. Nadolsky et al., "Implications of CTEQ global analysis for collider observables", *Phys. Rev.* **D78** (2008) 013004, arXiv:0802.0007. doi:10.1103/PhysRevD.78.013004.